ISSN 1063-7710, Acoustical Physics, 2011, Vol. 57, No. 6, pp. 779–786. © Pleiades Publishing, Ltd., 2011.
Original Russian Text © V.G. Andreev, T.B. Krit, O.A. Sapozhnikov, 2011, published in Akusticheskii Zhurnal, 2011, Vol. 57, No. 6, pp. 763–770.

NONLINEAR ACOUSTICS

Shear Waves in a Resonator with Cubic Nonlinearity

V. G. Andreev, T. B. Krit, and O. A. Sapozhnikov

Chair of Acoustics, Physical Faculty, Moscow State University, Moscow, 119991 Russia
e-mail: timofey@acs366.phys.msu.ru

Received March 2, 2011

Abstract—Shear waves with finite amplitude in a one-dimensional resonator in the form of a layer of a rubber-like medium with a rigid plate of finite mass at the upper surface of the layer are investigated. The lower boundary of the layer oscillates according to a harmonic law with a preset acceleration. The equation of motion for particles in a resonator is determined using a model of a medium with a single relaxation time and cubical dependence of the shear modulus on deformation. The amplitude and form of shear waves in a resonator are calculated numerically by the finite difference method at shifted grids. Resonance curves are obtained at different acceleration amplitudes at the lower boundary of a layer. It is demonstrated that, as the oscillation amplitude in the resonator grows, the value of the resonance frequency increases and the shape of the resonance curve becomes asymmetrical. At sufficiently large amplitudes, a bistability region is observed. Measurements were conducted with a resonator, where a layer with the thickness of 15 mm was manufactured of a rubber-like polymer called plastisol. The shear modulus of the polymer at small deformations and the nonlinearity coefficient were determined according to the experimental dependence of mechanical stress on shear deformation. Oscillation amplitudes in the resonator attained values when the maximum shear deformations in the layer were 0.4–0.6, which provided an opportunity to observe nonlinear effects. Measured dependences of the resonance frequency on the oscillation amplitude corresponded to the calculated ones that were obtained at a smaller value of the nonlinear coefficient.

Keywords: rubber-like materials, cubic nonlinearity, mechanical resonator.

DOI: 10.1134/S1063771011050022

INTRODUCTION

The growing interest in wave processes in cubically nonlinear media is caused by the opportunity to use nonlinear effects for medical diagnostics of soft tissues [1]. Tissue elasticity in an affected region changes drastically, which provides an opportunity to reveal pathology by measuring the local velocity and attenuation of shear waves. The methods for noninvasive excitation and detection of shear waves that were proposed by different authors demonstrated the possibility of localization and determination of inhomogeneities in the shear modulus both in phantoms of biological tissues [2] and clinically [3, 4]. The nonlinearity of the shear modulus is also an informative parameter providing an opportunity to specify the diagnostic information obtained with linear measurements [5]. The nonlinear parameter of a medium can be obtained from both static measurements and measurements of parameters for nonlinear wave processes. A special feature of media with an inversion center (soft biological tissues may be also ascribed to them with good precision) is the absence of quadratic nonlinearity in the case of shear deformations. In these media the main contribution to development of nonlinear processes belongs to cubic nonlinearity.

Traveling waves of finite amplitude in media with cubic nonlinearity have been investigated in sufficient detail [6–8]. It is has been shown that, in a cubically nonlinear medium, the profile of a wave harmonic at the input is distorted symmetrically in the process of propagation and acquires, at a certain distance, a trapezoidal shape with steep fronts. Analytical expressions were obtained in [9] for spectral characteristics of a simple wave in a cubically nonlinear medium both at the stage of its transformation from a sinusoidal form to formation of profile discontinuity and for an asymptotically self-similar profile in the form of a "trapezoidal saw." The results of experimental observation for dynamics of nonlinear transformation for the profile of a harmonic wave in a gel-like medium are described in [10], where both the wave profiles at different distances from the source of shear waves and their harmonic composition are given. The authors of [10] proposed to use the acousto-elastic effect, i.e., the dependence of elastic wave velocity on the static deformation of a medium, to measure the nonlinear elasticity moduli of gel-like media with a small value of the shear modulus. Theoretical fundamentals for determination of a limited number of nonlinear constants in incompressible media are described in [7, 11, 12]. The results of measuring nonlinear constants in

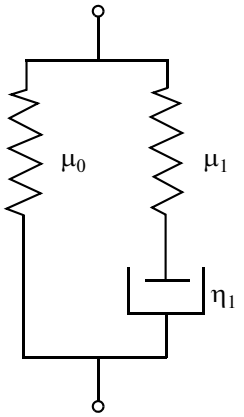

Fig. 1. A mechanical model for a rubber-like medium with a single relaxation time.

samples made of a gelatin–agar composition are given in [13, 14].

Standing waves in cubically nonlinear media are analyzed now in less detail, although they are not less interesting both as an object for fundamental research and from the point of view of practical applications. The theoretical analysis of standing wave behavior in a cubically nonlinear medium is conducted in [15], where solutions for waves with shock fronts are obtained. Review [16] considers in detail the models and approximate methods for analyzing standing waves in resonators in conditions of strongly pronounced nonlinearity. Wave analysis is performed for media with quadratic and cubic nonlinearity and for the nonlinearity arising due to boundary mobility.

To excite standing waves with finite amplitudes, it is convenient to use a resonator in the form of a plane-parallel layer of a rubber-like material with a rigid plate fixed at its upper boundary. The resonator thickness is selected in such a way that about a quarter wavelength would fit it. It is demonstrated in [17] that standing waves arise in this resonator. Their amplitudes are one order of magnitude or more larger than the amplitude of displacements applied to the lower boundary of the resonator even in the case of use of a polymer material with a large shear viscosity. A plastisol polymer material (its manufacturer is the company M-F Manufacturing, United States) is used as a medium with cubical nonlinearity. Its nonlinear parameter was determined from the static dependence of shear deformation on stress [18]. This work is devoted to experimental investigation of standing shear waves excited in a resonator filled with a medium with cubic nonlinearity. Waves of moderate amplitude are analyzed in which shock fronts are not yet formed. In this case an approach based on the model of a one-dimensional resonator is developed [17, 19].

CALCULATION OF STANDING WAVES IN A ONE-DIMENSIONAL RESONATOR WITH CUBIC NONLINEARITY

Let us consider a resonator in a form of a rubber-like sample shaped as a rectangular parallelepiped with the height L and horizontal facets with the area S. The lower facet of the sample is fixed to a rigid horizontal plate oscillating harmonically under the action of a driving force in the horizontal direction along the x axis. Another rigid plate with the mass M and an area equal to the area of the upper facet S is fixed at the upper facet ($y = L$). There is no slipping between the plates and the horizontal facets of the sample. It is assumed that the resonator thickness L is much smaller than the transverse dimensions. This assumption provides the opportunity to consider that particle motion depends only on the vertical coordinate; i.e., it is possible to use a one-dimensional approximation. It is demonstrated in [20] that this model of a one-dimensional resonator describes sufficiently exactly the behavior of a resonator with finite dimensions if the resonator thickness does not exceed the quarter of the length in the direction x.

A model taking into account dissipative processes in the simplest approximation, in which mechanical stress is represented in the form of an elastic addend directly proportional to deformation and a viscous addend directly proportional to the deformation rate (the Kelvin-Voigt rheological model), is used in [17] to investigate theoretically linear oscillations in the above resonator. It turned out that, in the case of the corresponding selection of parameters, the model provided an opportunity to describe well the observed resonance curves, but, in the case of proceeding to the resonances of higher orders, one has to decrease the model viscosity and increase the elastic modulus. In the linear case, this fitting of parameters in the vicinity of the investigated resonance is unnecessary, but in the nonlinear case higher harmonics arise; i.e., the process becomes wide-band and, therefore, the Kelvin-Voigt rheological equation of state is inapplicable and modification of it is necessary that takes into account the viscosity decrease and the increase of medium rigidity with the frequency growth. The simplest approach here is connected with introduction of relaxation processes [21, 22]. It is necessary also to modify the elastic element in the rheological model while considering nonlinear oscillations.

Let us consider a model medium in which a mechanical stress consists of a relaxation stress and an elastic stress directly proportional to deformation. The mechanical model of a medium is presented by a parallel connection of an elastic element with the nonlinear modulus $\mu_0 = \mu_{00}(1 + \beta\varepsilon^2)$ and the Maxwell viscoelastic element with the viscosity η_1 and the shear modulus $\mu_1 = \eta_1/\tau$ (see Fig. 1). Here $\varepsilon = \partial u/\partial y$ is shear deformation, u is the spring displacement, τ is the relaxation time, μ_{00} is the linear static shear modulus,

and β is the nonlinear parameter. In the case of deformation of the whole system for the value ε, a mechanical stress arises in it,

$$\sigma = \sigma_\infty + \sigma', \quad (1)$$

which consists of the spring stress

$$\sigma_\infty = \mu_0 \varepsilon = \mu_{00}\left(1 + \beta\varepsilon^2\right)\varepsilon \quad (2)$$

and the stress of the Maxwell scheme σ'. Let us express the Maxwell scheme stress through the deformation of a spring $\varepsilon_A = \sigma'/\mu_1$ and a damper ε_B, where $\partial\varepsilon_B/\partial t = \sigma'/\eta_1$. To do this we differentiate over time the expression for ε_A and add the result of differentiation to the expression for $\partial\varepsilon_B/\partial t$. In this case we take into account that the sum $\varepsilon_A + \varepsilon_B = \varepsilon$ is equal to the deformation of the whole Maxwell scheme, which is also equal to the spring deformation $\varepsilon = \sigma_\infty/\mu_0$. Then we can write down the following equation:

$$\frac{\partial\sigma'}{\partial t} + \frac{\sigma'}{\tau} = \frac{\eta_1}{\tau}\frac{\partial\varepsilon}{\partial t}, \quad (3)$$

where $\tau = \eta_1/\mu_1$ is the characteristic time of stress relaxation. It is necessary to note that, multiplying both parts of Eq. (3) by τ and performing a limiting transition at $\tau \to 0$, we obtain $\sigma'_{\tau\to 0} = \eta_1 \partial\varepsilon/\partial t$; i.e., the considered model transforms into the Kelvin-Voigt model that we used in [17].

To use Eq. (3) conveniently in a numeric form we write it down as follows:

$$\frac{\partial}{\partial t}\left(\sigma' e^{\frac{t}{\tau}}\right) = \frac{\eta_1}{\tau} e^{\frac{t}{\tau}}\frac{\partial v}{\partial y}. \quad (4)$$

It follows from Eq. (2) that the elastic part of stress

$$\frac{\partial\sigma_\infty}{\partial t} = \mu_{00}\left(1 + 3\beta\varepsilon^2\right)\frac{\partial v}{\partial y}. \quad (5)$$

In Eqs. (4) and (5), we introduced the vibrational velocity $v = \partial u/\partial t$ and took into account that $\varepsilon = \partial u/\partial y$.

The equation of motion for medium particles has the form

$$\frac{\partial v}{\partial t} = \frac{1}{\rho}\frac{\partial\sigma}{\partial y}. \quad (6)$$

Equations (4)–(6) must be complemented with boundary conditions. The first condition is a preset value of acceleration for the lower resonator plate, and the second one is determined from the law of motion for the upper plate,

$$\left.\frac{\partial v}{\partial t}\right|_{y=0} = W_0 \cos\omega t; \quad (7)$$

$$\left.\left(M\frac{\partial v}{\partial t} + \sigma S\right)\right|_{y=L} = 0. \quad (8)$$

The obtained system of relationships (1) and (4)–(8) was simulated by the finite difference method at shifted grids [23]. The operability of the numeric scheme written down was verified by comparing the calculated results with an analytical solution for a linear resonator ($\beta = 0$) that was obtained in [17]. In this case the relation of stress and deformation used in [17] was modified taking into account a model of a medium with a single relaxation time.

DESCRIPTION OF EXPERIMENTAL SETUP AND MEASURING TECHNIQUE

Measurements were conducted with two resonators shaped as rectangular parallelepipeds made of a polymer material called plastisol. A rigid plate with the mass M was fixed at the upper facet of the parallelepiped. The resonator thickness was the same for both resonators and constituted 15 mm. The length and width were 67 and 40 mm for resonator *I* and 70 and 40 mm for the resonator *II*. The masses of the upper plates were approximately equal (12 g for resonator *I* and 11.55 g for resonator *II*).

Measurements of the shear modulus for plastisol μ_0 were conducted in both resonators in the case of their static deformation [18]. To do this the lower boundary of a resonator was fixed and a certain force was applied to the upper plate, which produced shear stress in the layer. According to the approximation of a measured dependence of shear deformation on the applied stress by a cubic parabola, the linear shear modulus $\mu_{00} = 9.9 \pm 0.6$ kPa and the nonlinear parameter $\beta = 1.34 \pm 0.23$ for resonator *I* and $\mu_{00} = 6.7 \pm 0.4$ kPa and $\beta = 0.76 \pm 0.13$ for resonator *II* were determined.

The relaxation time and shear viscosity for the resonator material were determined from the frequency dependence of the upper plate acceleration measured in a linear mode in the frequency range 20–400 Hz. Oscillations of the lower resonator plate were excited by a Brüel&Kjær 4810 vibrator. An electrical signal was fed to the vibrator from a Tektronix 3021B signal generator through an MF LV 103 power amplifier. The accelerations of the upper and lower resonator plates were measured by Brüel&Kjær 4374 miniature uniaxial accelerometers. The mass of accelerometers was 1 g; i.e., their effect on the process of resonator oscillations was ignorable. Accelerometer signals were detected by a Tektronix 3032B digital oscilloscope and transmitted through a GPIB interface to a computer. Experimental setup control and data acquisition were performed using a computer code written in the LabView environment. In the process of measuring resonance curves, the acceleration of the lower resonator boundary was the same at each frequency and constituted 1 m/s^2 that corresponded to a linear mode of measurements. Measurements were conducted with the frequency step of 0.1 Hz that provided sufficient precision for determination of plastisol viscoelastic parameters. To provide constancy for the amplitude of the lower plate acceleration within the indicated frequency range, we used the following algorithm. At a preset frequency at the generator output, we set the voltage for the amplitude of the lower plate acceleration to be slightly smaller than the necessary value.

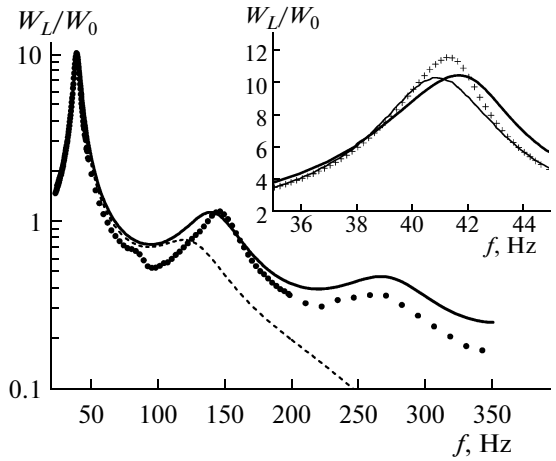

Fig. 2. Resonance curves obtained for resonator *I*. The basic plot represents resonance curves in a linear mode of oscillations ($W_0 = 1$ m/s^2). Dots indicate measured values, and the solid line is for the results calculated using the model of a medium with a single relaxation time. The dashed line shows the dependence calculated for a medium without relaxation. The insert shows the resonance curves in the region of the first resonance at the acceleration amplitude at the lower resonator boundary $W_0 = 15$ m/s^2. Symbols correspond to measured values, and calculated results are shown by a thick solid line. A thin line is for calculation for linear oscillations $W_0 = 1$ m/s^2).

This voltage increased up to the value, when the acceleration amplitude achieved the necessary value with an error no larger than 2%. Stationary oscillations developed in a resonator for 2–3 s; after that measurements and recording of the acceleration of the lower resonator plate were performed. Then the next frequency value was set and the measurements were repeated according to the described algorithm.

This algorithm has a fundamental value while studying resonance characteristics in a nonlinear mode when it is necessary to provide constancy for the external effect upon a resonator. However, in a nonlinear mode, the acceleration profile for the lower plate gets distorted because of generation of higher harmonics in a resonator. Therefore, in a nonlinear mode, a constant acceleration amplitude was maintained at the principal frequency that required modification of the above algorithm for measuring the resonance characteristics. A realization containing about 50 oscillation periods for the lower plate acceleration was recorded, and the amplitude of the principal harmonic was conducted by the FFT method. Then such an acceleration of the lower plate was selected by regulating the output voltage of the driving generator, when the preset level of amplitude at the principal frequency was attained with an error not exceeding 3%.

Measured properties of the resonators that were used for calculations

Resonator	μ_{00}, kPa	β	τ, ms	η_1, Pa · s
I	9.9 ± 0.6	1.34 ± 0.23	0.7 ± 0.2	4.7 ± 0.3
II	6.7 ± 0.4	0.76 ± 0.13	1.2 ± 0.3	2.8 ± 0.2

RESULTS OF MEASUREMENTS AND THEIR COMPARISON WITH NUMERICAL CALCULATION

An experimental dependence for the acceleration ratio for the upper and lower resonator plates that corresponds to the linear mode of oscillations in resonator *I* is given in Fig. 2 by dots. Numerical calculation for the linear mode was conducted using the model of a medium with a single relaxation time and at zero nonlinear coefficient. The values of the relaxation time and the coefficient of shear viscosity varied in the process of calculation so as to obtain the best (in the sense of the minimal root-mean-square deviation) coincidence of experimental and calculated dependences (demonstrated by a solid line in Fig. 2) in the range 20–200 Hz. Thus the values $\tau = 0.7$ ms and $\eta_1 = 4.7$ Pa · s were determined. It is necessary to note that, in the frequency range 10–300 Hz, where the three first resonance frequencies of the investigated resonator lie, plastisol has strongly pronounced dispersion properties. This can be seen well from comparison of experimental results with the form of the resonance curve (a dashed line) calculated according to the Kelvin-Voigt model, where the parameters of plastisol $\mu = 9.88$ kPa and $\eta = 4.7$ Pa · s do not depend on frequency. This curve coincides with the experimental one in the region of the first resonance, but, at high frequencies, the experimental dependence differs strongly: the frequencies of the measured second and third resonances lie higher, which is evidence of increase of plastisol elasticity with the growth of frequency, while the amplitude of the measured resonances is higher, which is connected with decrease of viscosity with the frequency growth. The values of relaxation time $\tau = 1.2$ ms and the coefficient of shear viscosity $\eta_1 = 2.8$ Pa · s were obtained for resonator *II* in an analogous way. The resonator parameters used for calculation are given in the table.

Figure 3 gives the results of calculation for resonance curves for resonator *I* near the first resonance frequency at different values of the acceleration amplitude for the lower plate W_0. At each value of W_0 a resonance curve was calculated first at a slow increase of frequency and then, at its slow decrease. At the initial time moment the value of the amplitude W_0 and the minimal frequency were set. Then the frequency was increased at the rate 0.1 Hz/s. In this case the acceleration of the upper plate W_L was recorded each second and the amplitude of the first harmonic was calculated. Calculation of a resonance curve at decreasing frequency was conducted analogously. The difference was only the fact that at the initial time moment the

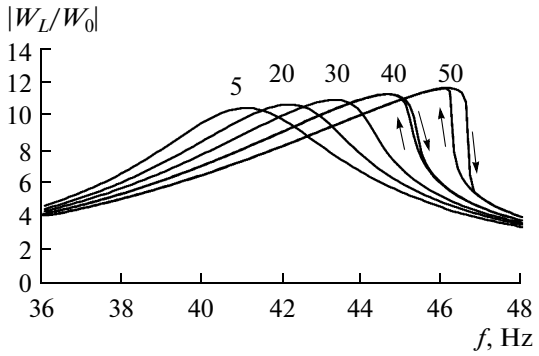

Fig. 3. Resonance curves near the first resonance frequency that are calculated at different amplitude values for the acceleration of the lower plate W_0 in resonator *I*. Numbers by the curves correspond to the amplitude W_0 in meters per second squared. Arrows indicate the direction of frequency variation in the process of calculation.

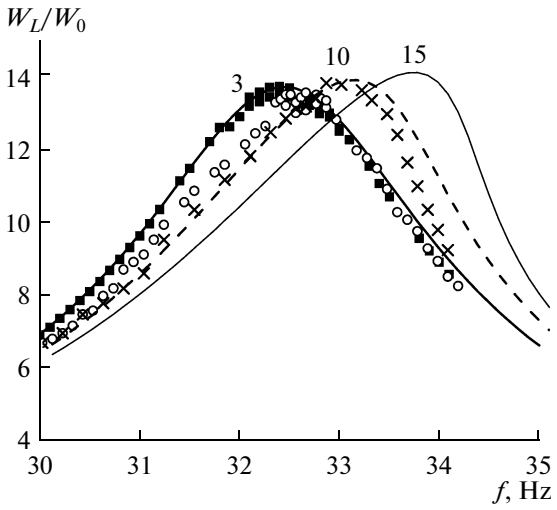

Fig. 4. Resonance curves near the first resonance frequency that are obtained for resonator *II* at different amplitude values for the acceleration of the lower plate W_0. The results of measurements are indicated by symbols (■ is for $W_0 = 3$ m/s^2, ○ is for $W_0 = 10$ m/s^2, and × is for $W_0 = 15$ m/s^2) and the calculated dependences by lines. Numbers by the curves correspond to the amplitude W_0 in meters per second squared.

value of the maximum frequency was set. In the linear oscillation mode ($W_0 \le 5$ m/s^2) the acceleration amplitude for the upper resonator boundary increases by 10.5 times in comparison with the amplitude at the lower boundary that was set by the vibrator. At the lower plate acceleration of 30 m/s^2, the velocity amplitude at the upper resonator boundary attains V_L = 1.2 m/s, which constitutes 39% of the shear wave velocity. At these particle velocities in a resonator, nonlinear effects manifest themselves. The resonance becomes asymmetrical, and the resonance frequency increases. The acceleration gain factor also increases in comparison with the linear case and attains 11.6 at $W_0 = 50$ m/s^2. At the amplitudes $W_0 > 40$ m/s^2, the resonance curves obtained for increasing frequency and its decrease (indicated by arrows) do not coincide; i.e., a bistability region arises. As the oscillation amplitude in a resonator grows, the bistability region widens. The effect of asymmetry for a resonance curve and the shift of the resonance frequency were observed experimentally. Crosses in the insert in Fig. 2 show the results of measuring a resonance curve at W_0 = 15 m/s^2. The results of resonance curve calculation in the linear case and for $W_0 = 15$ m/s^2 are given there also. An increase of the first resonance frequency for 0.4 Hz is observed that is smaller than the calculated value almost two times (0.7 Hz). Amplification of the oscillation amplitude at the upper resonator boundary in the resonance was 11.7 in the experiment that exceeded the calculated value of 10.6 almost for 10%.

Nonlinear effects are stronger in resonator *II* made of the polymer with a smaller coefficient of shear viscosity. In the mode of linear oscillations, the acceleration amplitude for the upper boundary of the resonator *II* increases by 13.7 times in comparison with the amplitude at the vibrator (see Fig. 4). A comparatively small viscosity is the reason that nonlinear effects in resonator *II* to manifest themselves already at the acceleration amplitudes at the lower plate exceeding 5 m/s^2. The bistability region in calculated curves arises at $W_0 = 20$ m/s^2. Measured resonance curves at different accelerations of the lower resonator (*II*) plate are indicated in Fig. 4 by various symbols. One can see that the resonance curves become asymmetrical and the resonance frequency grows with the increase of oscillation amplitude in the resonator. The results of more detailed measurements for increasing resonance frequency with growth of the acceleration amplitude at the lower boundary W_0 are demonstrated in Fig. 5. Here the solid line gives the results for the nonlinear parameter value $\beta = 0.76$ obtained from static measurements. According to the calculation, the resonance frequency must increase almost twice as fast as it was measured in the experiment. The dashed line shows the calculation results for the value $\beta = 0.35$, when the deviation from experimental data was minimal.

The stabilization time for a stationary mode of oscillations in the bistability region may exceed significantly the characteristic times in the mode of linear oscillations. The acceleration profiles near the resonance frequency were calculated for 30 s after switching on of the acceleration constant in the amplitude at the lower plate of resonator *II*. Calculation was conducted at different amplitudes of the lower plate acceleration. At acceleration amplitudes smaller than 15 m/s^2, the stabilization time of oscillations does not depend on the amplitude and constitutes about ten periods at frequencies near the resonance (32–34 Hz). At the amplitudes of 20 and 25 m/s^2, the stabilization time for a stationary mode increases and, in this case,

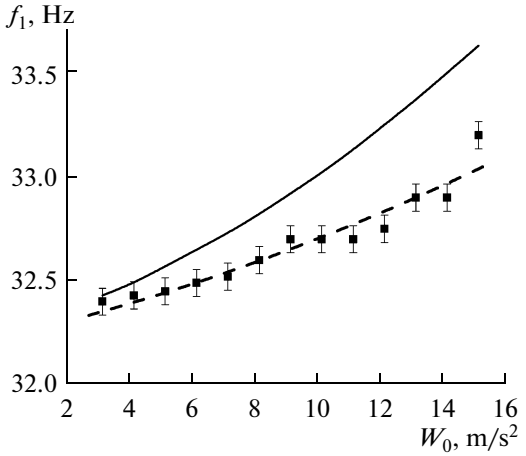

Fig. 5. Dependence of the first resonance frequency on the acceleration amplitude at the lower plate of resonator *II*. Symbols correspond to measured values, and solid and dashed lines show the results of calculation for $\beta = 0.76$ and $\beta = 0.35$, respectively.

its value depends on frequency. At the resonance frequency and the acceleration amplitude at the lower plate $W_0 = 25$ m/s^2, the stationary mode stabilizes during 15 periods. In the bistability region, stabilization of a stationary mode at the indicated amplitude W_0 needs more time. The longest stabilization time (120 periods) for a stationary mode is at the frequency of 35.5 Hz corresponding to the middle of the bistability region. At the frequency of 35.7 Hz, the stabilization time is already three times shorter and constitutes about 1 s (40 periods).

Propagation of a harmonic wave with a finite amplitude in a medium with cubic nonlinearity leads to generation of harmonics and distortion of the initial sinusoidal profile. Figure 6 shows measured and calculated acceleration profiles at the upper plate of resonator *I* at the resonance frequency and the amplitude $W_0 = 15$ m/s^2. The profiles almost coincide and differ little from the profile of a harmonic wave that is connected with a large attenuation for both the wave at the principal frequency and the wave of the third harmonic. It is possible to determine from linear measurements (Fig. 2) that the ratio W_L/W_0 at the frequency of the third harmonic (123 Hz) is smaller than 1 and constitutes 0.7 (measured) and 0.94 (calculated). Thus, there is no resonance amplification of the third harmonic in this resonator. If we reduce the viscosity, nonlinear effects become more strongly pronounced. Figure 6 demonstrates the profile calculated for the case of small viscosity ($\eta = 1.6$ Pa · s). One can see well the distortions of this profile that are associated with generation of the third harmonic.

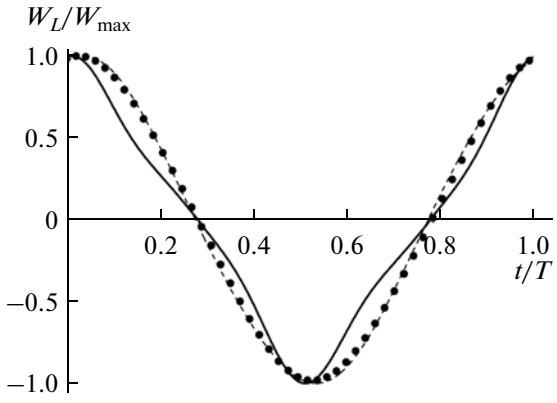

Fig. 6. Time profile of acceleration at the upper plate of resonator *I* at the resonance frequency at $W_0 = 15$ m/s^2. The measured and calculated profiles are indicated by dots and a dashed line, respectively. The solid line shows the calculated profile for a resonator with the coefficient of shear viscosity $\eta = 1.6$ Pa · s.

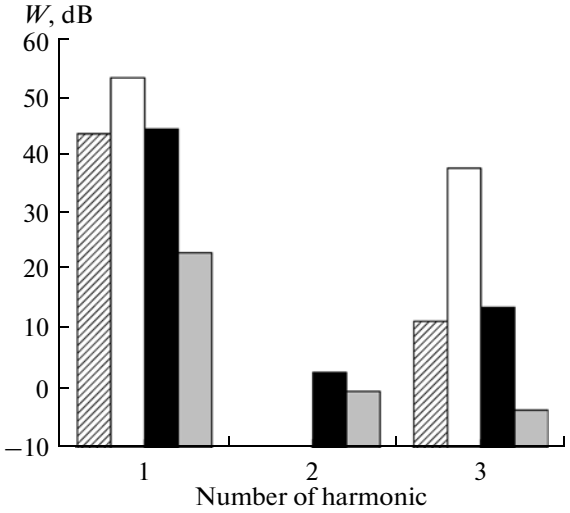

Fig. 7. The first three harmonics of acceleration at the upper plate of resonator *I* at the acceleration amplitude at the lower plate of 15 m/s^2 at the resonance frequency. Black and gray colors indicate the harmonics of measured acceleration at the upper (W_L) and lower (W_0) plates of the resonator. The shaded and white columns correspond to the harmonics of the acceleration W_L that are calculated for resonators with the coefficients of shear viscosity $\eta = 4.7$ and 1.6 Pa · s, respectively.

Figure 7 gives the results of harmonic analysis for the time profiles demonstrated in Fig. 6. When the viscosity of a medium is sufficiently large ($\eta = 4.7$ Pa · s), the level of the third harmonic in a resonator is small and constitutes −32 dB with respect to main harmonic, which corresponds to the results of measurements. If the viscosity coefficient decreases to 1.6 Pa · s, the level of the third harmonic grows for 16 dB and constitutes −15 dB with respect to the fundamental harmonic. This efficiency increase for generation of the third harmonic is explained by both the growth of the fundamental harmonic amplitude for 10 dB and the resonance amplification of the third harmonic in a

resonator (the ratio W_L/W_0 at the frequency of the third harmonic is equal to 1.9). It is necessary to note that, in the measured spectrum of acceleration at the lower plate, the second and third harmonics are present but their level is low (−23 and −26 dB, respectively) in comparison with the level of the fundamental harmonic.

CONCLUSIONS

Manifestation of nonlinear effects and the process of harmonics' generation in a resonator filled with a medium with cubic nonlinearity has several special features. In a resonator tuned to the resonance frequency of the fundamental harmonic, the waves of higher harmonics arising due to cubic nonlinearity are not resonant. This is caused by the dispersion of shear wave velocity in the low-frequency range induced by the finite relaxation times of viscoelastic parameters in a medium. The presence of a rigid plate with a finite mass at the upper boundary of a resonator also leads to shifting resonance frequencies and desynchronizing the waves of the fundamental frequency and their harmonics [17]. Therefore, generation of the third and higher harmonics does not occur in the resonance mode. In particular, the amplitude of particle velocity for the third harmonic can be estimated proceeding from a relation obtained in [7] for the case of a traveling wave,

$$V_3(y) = \frac{\beta_Z \omega V_0^3}{24 c_t^3 \alpha}\left(e^{-3\alpha y} - e^{-9\alpha y}\right), \quad (9)$$

where V_0 is the amplitude of particle velocity for a wave at the fundamental frequency ω, $\beta_Z = 1.5\beta$ is the nonlinear parameter of a medium, $c_t = (\mu/\rho)^{1/2}$ is the velocity of a shear wave), and $\alpha = \dfrac{\eta\omega^2}{2\rho_0 c_t^3}$ is the attenuation coefficient for a wave at the fundamental frequency. The acceleration amplitude for the third harmonic at the upper resonator boundary that arises at a single transmission through the resonator thickness L can be written down in the form

$$W_3(y = L) = \frac{\beta W_L^3}{16\omega c_t^3 \alpha}\left[\exp(-3\alpha L) - \exp(-9\alpha L)\right]. \quad (10)$$

Thus, the amplitude of the third acceleration harmonic depends cubically on the acceleration amplitude for a wave at the fundamental frequency. The amplitude of the fundamental harmonic in a resonator with small viscosity (η = 1.6 Pa · s) is three times higher than that in a resonator with the viscosity η = 4.7 Pa · s (see Fig. 7), which, according to [7], must lead to increasing the amplitude of the third harmonic for 29 dB, which is very close to the result (26 dB) obtained by simulation. The amplitude of the third harmonic in resonators with different shear viscosities is affected by the possibility of amplification due to resonance. In a resonator with a small viscosity, the third harmonic can be amplified additionally due to resonance 1.9 times, while for a resonator with a large viscosity this amplification is absent (see Fig. 2). This means that viscosity reduction in a medium is a determining factor for increase in efficiency for nonlinear processes in the considered resonators.

Our results show that one can observe the effect of resonance frequency increase with the growth of oscillation amplitude in a resonator with a cubically nonlinear medium. According to calculation, nonsymmetrical distortion of the resonance curve shape happens. However, there is no quantitative correspondence for the effects observed in the experiment and the results of calculations performed with the parameters determined from static measurements. For example, growth of the first resonance frequency at a preset value for the coefficient of shear viscosity corresponds to calculated values for the nonlinearity coefficient $\beta = 0.35$, which is less than half the value determined from static measurements. Our measurements demonstrated that the linear static and dynamic moduli of elasticity for a rubber-like polymer differ. As frequency grows, the linear shear modulus increases, which leads to nonequidistance of resonance frequencies. It is possible to assume that the values of the static and dynamic nonlinearity coefficients also differ. This fact could be taken into account by a complication of a rheological model (Fig. 1), for example, assuming a spring in the Maxwell scheme to be nonlinear, being softened with the growth of deformation, $\mu_1 = \mu_{10}\left(1 - \beta_1\varepsilon^2\right)$. It is necessary to note that there is now a rather agitated discussion in the literature with respect to determining the elastic parameters of incompressible materials, to which many polymers and soft biological tissues belong. Both theoretical models for describing these media with the help of a limited number of nonlinear parameters [7, 11, 12] and the techniques for measuring these parameters [13] are proposed. The method of an interferometer with its use in a nonlinear mode that is proposed here can be useful for acquiring information on nonlinear parameters of rubber-like media in the low-frequency range.

ACKNOWLEDGMENTS

This work was supported by the Russian Foundation for Basic Research and the International Scientific and Technological Center, project no. 3691.

REFERENCES

1. A. A. Oberai, N. H. Gokhale, S. Goenezen, P. E. Barbone, T. J. Hall, A. M. Sommer, and J. Jiang, Phys. Med. Biol. **54**, 1191 (2009).
2. V. G. Andreev and A. V. Vedernikov, Vestn. Mosc. Univ., Ser. Fiz. Astron. **4** (3), 52 (2006).
3. M. Tanter, J. Bercoff, A. Athanasiou, T. Deffieux, J.-L. Gennisson, G. Montaldo, M. Muller, A. Tardi-

von, and M. Fink, Ultrasound Med. Biol. **34**, 1373 (2008).

4. B. S. Garra, I. Cespedes, J. Ophir, S. Pratt, R. Zuubier, and C. M. Magnat, Radiology **202**, 79 (2002).
5. R. Q. Erkamp, S. Y. Emelianov, A. R. Skovoroda, and M. O'Donnell, IEEE Trans. Ultrason. Ferroelectr. Freq. Control **51**, 532 (2004).
6. O. V. Rudenko and O. A. Sapozhnikov, Zh. Eksp. Teor. Fiz. **106**, 395 (1994) [JETP **79**, 220 (1994)].
7. E. A. Zabolotskaya, M. F. Hamilton, Y. A. Ilinskii, and G. D. Meegan, J. Acoust. Soc. Am. **116**, 2807 (2004).
8. M. S. Wochner, M. F. Hamilton, Yu. A. Ilinskii, and E. A. Zabolotskaya, J. Acoust. Soc. Am. **123**, 2488 (2008).
9. V. A. Gusev and Yu. N. Makov, Akust. Zh. **56**, 591 (2010) [Acoust. Phys. **56**, 626 (2010)].
10. S. Catheline, J.-L. Gennisson, M. Tanter, and M. Fink, Phys. Rev. Lett. **91**, 43011 (2003).
11. M. Destrade, M. D. Gilchrist, and G. Saccomandi, J. Acoust. Soc. Am. **127**, 2759 (2010).
12. M. Destrade, M. D. Gilchrist, and R. W. Ogden, J. Acoust. Soc. Am. **127**, 2103 (2010).
13. M. Rénier, J.-L. Gennisson, C. Barrière, et al., Appl. Phys. Lett. **93**, 101912 (2008).
14. J.-L. Gennisson, M. Rénier, S. Catheline, C. Barrière, J. Bercoff, M. Tanter, M. Fink, J. Acoust. Soc. Am. **122**, 3211 (2007).
15. O. V. Rudenko, K. M. Hedberg, and B. O. Enflo, Akust. Zh. **53**, 522 (2007) [Acoust. Phys. **53**, 455 (2007)].
16. O. V. Rudenko, Acoust. Phys. **55**, 27 (2009).
17. V. G. Andreev, T. B. Krit, and O. A. Sapozhnikov, Akust. Zh. **56**, 190 (2010) [Acoust. Phys. **56**, 168 (2010)].
18. V. G. Andreev and T. A. Burlakova, Akust. Zh. **53**, 50 (2007) [Acoust. Phys. **53**, 44 (2007)].
19. V. G. Andreev, T. B. Krit, and O. A. Sapozhnikov, Akust. Zh. **56**, 579 (2010) [Acoust. Phys. **56**, 605 (2010)].
20. V. G. Andreev, T. B. Krit, V. V. Kostikov, et al., Akust. Zh. **57**, 3 (2011) [Acoust. Phys. **57**, 1 (2011)].
21. I. G. Mikhailov, V. A. Solov'ev, and Yu. P. Syrnikov, *Principles of Molecular Acoustics* (Nauka, Moscow, 1964) [in Russian].
22. J. Oudry, C. Bastard, V. Miette, R. Willinger, and L. Sandrin, Ultrasound Med. Biol. **35**, 1185 (2009).
23. O. A. Sapozhnikov, A. D. Maxwell, B. MacConaghy, and M. R. Bailey, J. Acoust. Soc. Am. **112**, 1190 (2007).

Translated by M.L. Lyamshev